Proceedings World Geothermal Congress 2020+1
Reykjavik, Iceland, April - October 2021

Performance evaluation of borehole thermal energy storage through energy and exergy analysis

Alberto Lazzarotto, Willem Mazzotti Pallard, Mohammad Abuasbeh and José Acuña

KTH, Department of Energy Technology, Brinellvägen 68, 100 44 Stockholm, Sweden

alberto.lazzarotto@energy.kth.se

Keywords: borehole thermal energy storage, performance, exergy analysis

ABSTRACT

The use of densely populated fields of borehole heat exchangers is a viable solution for seasonal thermal energy storage and has great potential to increase the share of renewable as well as temperature and exergy. These parameters are evaluated at the interface of the storage, e.g. inlet and outlet quantities, but also within the storage volume. An analytical model based on the line source is utilized to describe the heat transfer within the ground. The model provides the temperature field within the ground volume as a function of time and enables monitoring how the energy stored loses quality, i.e. exergy, as the difference between a given time of interest and the time of injection increases. The analysis proposed aims at breaking down the storage process in the borehole and evaluate how a variety of parameters in the configuration and operation of the system affect the processes of injection, storage and extraction of thermal energy. A set of test cases where a number of design and operational parameters are investigated is presented to illustrate the benefit and insight provided by the analysis.

1. INTRODUCTION

Energy storage will most likely play a crucial role in future, renewable-powered energy systems, due to increased intermittency of production plants, increased interplay between different systems and more decentralized energy prosumption (Chu & Majumdar, 2016; Mohd et al. , 2008;Moriarty & Honnery, 2016; Pickard, 2014). Most of the stored energy is meant for electricity production, mostly through pumped hydro storages that represent about 98% of the total amount of energy stored globally (Aneke and Wang, 2016; Dunn et al., 2011). As for thermal energy storages (TES), they only account for about 1% of the total energy stored (Aneke and Wang, 2016).

It is not surprising that heat is not the preferred form of storage considering that it is, in general, a less useful form of energy: irreversibility in thermodynamic processes usually emerge as heat (e.g. friction). It does not mean, however, that heat is a useless form of energy. Dinçer and Rosen (2010) state that when there is a mismatch between thermal energy supply and demand, e.g. in solar thermal installations, TES is the most direct way to store energy since it avoids unnecessary conversion processes. According to Forman et al. (2016), about half of the global energy production is wasted as heat, more than 60% of which is wasted at temperature below 100°C. Recovering part of this wasted heat would contribute in reducing CO_2 emissions but this would require a match between supply and demand, unless TES are used.

For high-latitude locations, seasonal TES are particularly attractive because there is usually a positive mismatch between supply and demand during summertime while this mismatch is negative wintertime (or vice versa, e.g. for cooling). Because seasonal TES should have large capacities and, thus, large volumes, it is common to find underground seasonal TES. Although it might not be the most efficient solution, the storage media is free and does not take any surface area.

This paper focuses on a common kind of underground TES, the Borehole TES (BTES) – i.e. storage of sensible heat in rock or soil through Borehole Heat Exchangers (BHEs). BTES have large storage capacities and the cost per amount of energy supplied is at the low-end compared to other TES solutions (see Table 3.3 in Dinçer & Rosen, 2011). Gehlin (2016) gives a comprehensive description of the technology providing definitions and a discussion on high temperature (up to 90°C) and low temperature (close to undisturbed ground temperature) BTES systems (Gehlin, 2016). A rather complete collection of data on existing high temperature storage is provided by Malmberg et al. (2018) and in the report by Kallesøe et al. (2019). Gehlin states that the development of high temperature BTES has decreased after an initial enthusiastic decade in favor of low temperature BTES. However, she also mentions that in recent years there is again a new interest in this technology for seasonal storage of solar heat, industrial waste heat and waste heat from cogeneration plants. This interest is shown also by current research projects such as the EU project Heatstore and the Swedish national program Termiska Energilager (https://www.energiforsk.se/program/termiska-energilager/) which started with the objective of accelerating the theoretical and practical development of the high temperature BTES. This work is part of the latter program and has the objective of investigating performance indicators for borehole energy storage system.

Performance of BTES are often presented in literature in terms of the so called energy efficiency η, which is the ratio between the energy extracted during the discharging season and the energy injected during the charging season. Another figure that is utilized, although less frequently, is the exergy efficiency ψ, which is a dual definition of η in terms of exergy. Exergy has the benefits of taking into account both the quantity of the heat exchanged as well as its ‘‘quality’’ which depends on the temperature of the heat. This paper aims at exploring performance indicators for the analysis of high temperature BTES. Six test cases corresponding to different configurations and system operations are simulated. Figures depending on temperature, energy, and exergy are evaluated at the interface of the storage, e.g. inlet and outlet quantities, but also within the storage volume.

2. METHODOLOGY

This section introduces the model that was implemented to perform borehole storage simulation as well as the performance indicators utilized for the analysis.

2.1 The model

The model used in this study is designed to simulate a borehole storage system operated by circulating a fluid inside an array of BHEs. The array consists of several hydraulic loops connected in parallel such that each loop is provided with the same inlet temperature. The model enables evaluating the performance of BTES systems given the bore field geometry and hydraulic arrangement (Cimmino, 2018; Lazzarotto, 2014). Figure 1 shows the application that is considered in this paper: 8 separate (non-identical) loops are fed in parallel with constant inlet mass flow at 90 °C during the summer and 55 °C during the winter. The borehole configuration and the arrangement studied are the ones of an actual pilot borehole storage (Tordrup et al., 2017). The system is fed from the internal borehole during summer and from the external boreholes during winter. The output temperature and the heat exchanged by the system are not directly imposed and are the result of the specific borehole configuration and operational strategy.

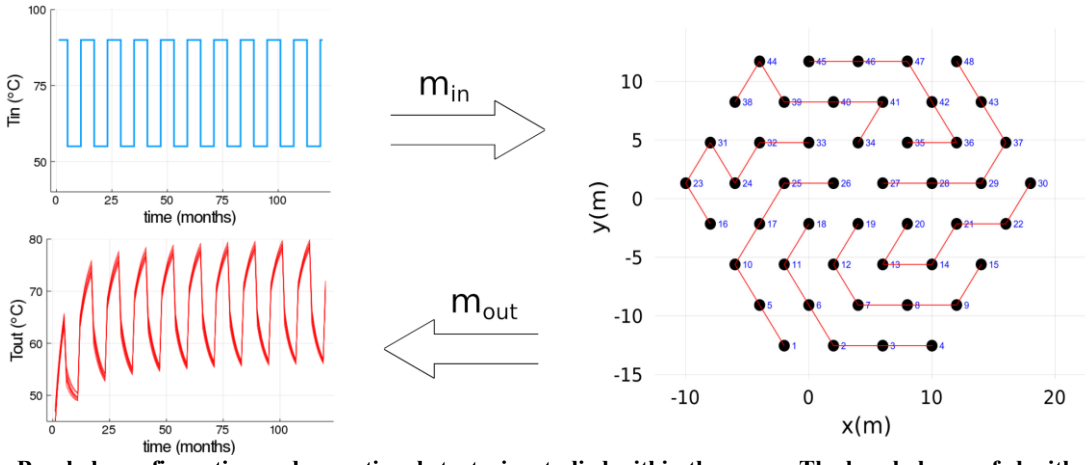

Figure 1: Borehole configuration and operational strategies studied within the paper. The boreholes are fed with mass flow at a temperature *Tin(t)*.

Modeling strategy

In this initial work, the ground is modeled as a two dimensional infinite solid by means of infinite line source solution (ILS). The choice of simulating a two dimensional model even though three dimensional models are readily available was made to simplify the methodology employed for the analysis presented in this work which requires to perform numerical integrations in control volumes (section 2.3). As a first step, it was therefore easier to develop the method for two dimensions.

Given a borehole storage with N boreholes the unknowns of the problems are the inlet temperature in the boreholes $T_{in}^{(i)}(t)$ [°C], the outlet temperature from the boreholes $T_{out}^{(i)}(t)$ [°C], the borehole wall temperature $T_b^{(i)}(t)$ [°C] and the power per meter exchanged by each borehole $q_b'^{(i)}(t)$ [W/m] for a total of 4N unknown at each time step in the simulation. The system can be modeled using a set of 4N linear equations that models the ground, the borehole, the interaction between the ground and the borehole and the topology of the hydraulic network.

Ground Model

$$T_b^{(i)}(t) - \frac{1}{2\pi k_g}\sum_{j=1}^{N} q'^{(j)}(t)\ \mathrm{g}(r_{j,i}, t_{\mathrm{step}}) = T_0 + \frac{1}{2\pi k_g}\sum_{k=1}^{N_t-1}\sum_{j=1}^{N}(q'^{(j)}(t_k) - q'^{(j)}(t_{k-1}))\ \mathrm{g}(r_{j,i}, t_{N_{t-1}} - t_k) \quad (1)$$

where k_g [W/m K] is the ground thermal conductivity, t [s] is time, $r_{j,i}$ [m] is the distance between borehole *i* and *j* in meters, and g is the thermal response factor which, as mentioned above, for the purpose of this paper is modeled using the ILS as showed in the following expression.

$$\mathrm{g}(r,t) = \mathrm{ILS}(r,t) = \frac{1}{2}\,\mathrm{E}_1\left(\frac{r^2}{4\alpha_g t}\right) \quad (2)$$

where E_1 is the exponential integral and α_g [m²/s] is the thermal diffusivity of the ground. It is worth noting that the term on the right hand side of equation 1 are values that can be computed given the load history of the storage. The equation is written to collect on the left hand side all the unknowns and the relative coefficients and, on the right hand side, the given terms. A similar style in presenting the model equations is adopted below since it provides a good idea of the relative matrix representation, which is then implemented to solve the model.

Borehole Model

The borehole has been modeled according to the method introduced by Cimmino (2016). The model is fairly general and can be applied to step-wise constant borehole temperature. In this initial work, we consider only the simple case of uniform borehole temperatures. The equation used in this paper is of the following form.

$$a_{\mathrm{in}}T_{\mathrm{in}} + a_{\mathrm{out}}T_{\mathrm{in}} + a_{\mathrm{b}}T_{\mathrm{b}} = 0 \tag{3}$$

For brevity in equation 3, we only report the linear relationship between T_{in}, T_{out} and T_{b}. The formulation for the coefficients a_{in}, a_{out} and a_{b} can be found in the reference article (Cimmino, 2016).

Heat Balance in the borehole

$$\dot{m}\, c_{p_f}\, T_{\mathrm{in}}^{(i)}(t) - \dot{m}\, c_{p_f}\, T_{\mathrm{out}}^{(i)}(t) - q_b'^{(i)}(t)\, H = 0 \tag{4}$$

where m [kg/s] is the mass flow rate in a loop, c_{pf} [J/(kg K)] is the specific heat of the fluid and H [m] is the length of the boreholes in meters.

Temperature constraint: hydraulic topology

Eq. 5 allows to impose the outlet to a value $f(t)$ while eq. 6 allows connecting the outlet of borehole j to the inlet of borehole i. These two constraints enable any possible hydraulic topology for the system.

$$T_{in}^{(i)}(t) = f(t) \tag{5}$$

$$T_{\mathrm{in}}^{(i)} - T_{\mathrm{out}}^{(j)} = 0 \tag{6}$$

Equations 1, 3, 4, 5 and 6 can be expressed in matrix form as system of equation $Ax = b$ with 4N equation and 4N unknowns. The system is fairly flexible, and we can build several matrices A corresponding to different topology and operation. This enables for instance switching flow direction during operation which may be desirable feature when studying borehole connected in series.

2.3 Performance indicators

The performance of the borehole storage are evaluated both at a system level (inlet-outlet) on a seasonal basis but also within the storage volume at any time t. Performance are evaluated both in terms of energy and exergy. For exergy calculation the temperatures are absolute temperatures expressed in Kelvin and the reference temperature T_0 considered is the undisturbed temperature of the ground equal to 281.15 K.

Seasonal system performance indicators

$$\eta \;=\; \frac{Q_d}{Q_c} = \frac{\int_{\tau_c}^{\tau_c+\tau_d} \dot{m}c_p\,(T_{\mathrm{out}}(t) - T_{\mathrm{in}})\,dt}{\int_0^{\tau_c} \dot{m}c_p\,(T_{\mathrm{in}}(t) - T_{\mathrm{out}})\,dt} \tag{7}$$

$$\psi \;=\; \frac{\mathrm{Ex}_d}{\mathrm{Ex}_c} = \frac{\int_{\tau_c}^{\tau_c+\tau_d} \dot{m}c_p \left[(T_{\mathrm{out}}(t) - T_{\mathrm{in}}(t)) - T_0 \ln\left(\frac{T_{\mathrm{out}}(t)}{T_{\mathrm{in}}(t)}\right)\right]\,dt}{\int_0^{\tau_c} \dot{m}c_p \left[(T_{\mathrm{in}}(t) - T_{\mathrm{out}}(t)) - T_0 \ln\left(\frac{T_{\mathrm{in}}(t)}{T_{\mathrm{out}}(t)}\right)\right]\,dt} \tag{8}$$

where Q [MWh] and Ex [MWh] stands respectively for heat and exergy, and the subscript 'c' and 'd' stand respectively for charging and discharging.

Storage performance indicator

$$\eta_{\mathrm{storage}}(V,t) = \frac{Q_{\mathrm{stored}}(V,t)}{Q_{\mathrm{exchanged}}(t)} = \frac{\int_V \rho_g c_{p_g}\,(T(\mathbf{x},T) - T_0)\,dV}{\int_0^t m_f c_{p_f}\,(T_{\mathrm{in}}(t) - T_{\mathrm{out}}(t))\,dt} \tag{9}$$

$$\psi_{\mathrm{storage}}(V,t) \;=\; \frac{\mathrm{Ex}_{\mathrm{stored}}(V,t)}{\mathrm{Ex}_{\mathrm{exchanged}}(t)} = \frac{\int_V \rho c_p \left[(T(\mathbf{x},t) - T_0) - T_0 \ln\left(\frac{T(\mathbf{x},t)}{T_0}\right)\right]\,dV}{\int_0^t \dot{m}c_p \left[(T_{\mathrm{in}}(t) - T_{\mathrm{out}}(t)) - T_0 \ln\left(\frac{T_{\mathrm{in}}(t)}{T_{\mathrm{out}}(t)}\right)\right]\,dt} \tag{10}$$

where Q_{stored} is the energy stored in the storage volume and $Q_{\mathrm{exchanged}}$ is the cumulative energy injected and extracted in to the BTES system. Similar definitions but in terms of exergy applies to Ex_{stored} and $Ex_{\mathrm{exchanged}}$. Since in this paper the model used to simulate the borehole storage is a two dimensional model Q_{stored} and Ex_{stored} are expressed in MWh/m. For this reason $Q_{\mathrm{exchanged}}(t)$ and $Ex_{\mathrm{exchanged}}(t)$ needs to be accordingly scaled by the length H of the boreholes. Seasonal parameters are presented in literature in several papers (Kizilkan and Dincer, 2012; Rosen et al., 2004; Rosen and Dincer, 2003; Sliwa and Rosen, 2017) and have been applied to borehole storage systems. The storage indicators have been used to optimize the operation of water tanks (Jack and Wrobel, 2009) but to the authors knowledge have not been used for borehole thermal storage application.

Other figures that are considered in this study are the fluid outlet temperature T_{out} and the mean storage temperature T_{storage}

$$T_{\mathrm{storage}}(V,t) = \frac{\int_V T(\mathbf{x},t)dV}{\int_V dV} \tag{11}$$

2.4 The storage volume

The evaluation of the storage performance requires the calculation of an integral over the storage volume. Unlike other storage systems such as water tanks where the identification of the storage volume is trivial, borehole systems are unbounded. The choice of a control volume for the storage is therefore not trivial and requires some definitions. In order to make a sensible choice for the boundary we considered a volume around the boreholes that contains a percentage 1-ϵ of the overall heat injected after a time τ_d corresponding to the time for the discharge cycle. We picked the discharging time as a reference time because it is the relevant time constant for extracting useful heat from the storage volume.

$$\frac{\mathrm{Q}_{\mathrm{stored}_{\epsilon,\tau_d}}(V_\epsilon,\tau_d)}{\mathrm{Q}_{\mathrm{injected}}(\tau_d)} = 1-\epsilon \tag{12}$$

For a single borehole case the radius r_ϵ of this region is the one satisfying the following expression.

$$\frac{1}{q^{'}\tau_d}\,\rho_g\,c_{p_g}\int_{r_\epsilon}^{+\infty}\frac{q^{'}}{4\pi k_g}\mathrm{E}_1\left(\frac{r^2}{4\alpha_g\tau_d}\right)2\pi r\,dr = \epsilon \tag{13}$$

where E_1 is the Exponential integral function. The value of r_ϵ can be easily computed numerically and is utilized within this paper to provide a reference value to define the storage region containing N sources at location (x_i, y_i) with $i=1,\ldots,N$. The procedure consists in determining the family of points (x, y) with minimum distance from the sources (x_i, y_i) equal to r_ϵ. Such region $V\epsilon_1,\tau_d$ with unknown $\epsilon_1 \leq \epsilon$ contains the storage volume $V\epsilon,\tau_d$ and guarantees that at most only a portion ϵ of the heat extracted during the discharging season is coming from the region outside $V\epsilon_1,\tau_d$

It is clear that not all the energy/exergy stored in $V\epsilon_1\tau_d$ is recoverable. On the other hand such definitions of storage efficiencies measure the capability of the BTES to maintain the energy injected/extracted in the surrounding of the borehole system at distance from which it can be partly discharged.

The integrals of equation 9 and 10 are finite since they represent the energy and exergy stored in the volume. On the other hand, the line sources are singularities and the evaluation of the integrand function at the source's location returns infinity. This problem is solved by using the fact that the integration point in Gauss quadrature schemes are never at edges of the integration domain. We can therefore build the discretization domain following this rule and make sure that sources are placed on the boundary of elements of the discretization. Once we adopt these precautions we can safely calculate the integrals 9, 10 and 11 using numerical integration routines.

An interesting exercise is the calculation of η_{stored} in the infinite region which provides a verification of the correctness of the implementation of the borehole model (eq. 1) since η_{stored} must be equal to 1, i.e. the energy injected in the ground must be stored somewhere in the ground since the model considered is an infinite solid. The integral can be performed by exploiting suitable change of variables such as $x = t/(1-t^2)$ that maps the unbounded domain $(-\infty,+\infty)$ to the finite domain $(-1,+1)$, or $x = a+t/(1-t)$ that maps the unbounded domain $(a,+\infty)$ to the finite domain $(0,+1)$. This test was performed and verified.

Table 1: Properties utilized to define the reference case configuration case 0.

Property	Symbol	Value	Units
borehole radius	r_b	0.0575	m
borehole length	H	100	m
ground conductivity	k_g	3	W/m K)
ground heat capacity	C_g	$1.875\cdot10^6$	J/(m^3 K)
grout conductivity	k_b	1.5	W/(m K)
grout heat capacity	C_b	$3.1\cdot10^6$	J/(m^3 K)
minimum boreholes distance	B	4	m
mass flow rate per loop	$\dot{m}$	0.5	kg/s
density fluid	ρ_f	1000	
specific heat capacity fluid	cp_f	4182	J/(kg K)
arrangement	-	series	-
inlet temperature summer time	$T_{\mathrm{in,s}}$	90	°C
inlet temperature winter time	$T_{\mathrm{in,w}}$	55	°C
Undisturbed temperature	T_0	8	°C

2.5 Test cases design

The configuration showed in figure 1 was used as a reference case. Table 1 gives an overview of the parameters utilized to model the ground and the boreholes. In the base case configuration, the boreholes are connected in series and, as previously mentioned, they are supplied with a temperature of 90 °C during summer and 55 °C during wintertime. A flow of 0.5 kg/s per loop is imposed and circulation goes from the center to the outer region of the boreholes during summer and in the opposite direction during wintertime, i.e. six months each. Simulations are performed with a monthly time step and for a time horizon of ten years. Modifications of all the properties provided in table 1 can be applied to compare the performance indicators presented for a large array of configurations. In this paper, as shown in table 2, only grout thermal conductivity, mass flow rate and borehole arrangement (parallel or series) were varied in order to illustrate the method.

Table 2: Definition of five case studies obtained by modifying the properties arrangement, grout thermal conductivity and mass flow rate per borehole. The underlined properties highlighted in red are the properties that have been changed compared to the reference case.

	arrangement	k_b (W/(mK))	$\dot{m}$ (kg/s)
case 0	series	1.5	0.5
case 1	parallel	1.5	0.5
case 2	series	2.5	0.5
case 3	parallel	2.5	0.5
case 4	series	2.5	1
case 5	parallel	2.5	1

3. RESULTS AND DISCUSSION

3.1 Temperatures analysis

The model described in section 2 was used to obtain the solutions for the temperatures T_i, T_o and T_b, and for the heat rates q_b' for the six test cases. These results (figures 2-7) are displayed for a set of boreholes located along a series connection in the base configuration. A color code is utilized to distinguish each individual borehole. For borehole in series (figure 2), the inlet temperatures T_i (solid thick lines) during summertime decrease from the highest value (equal to 90°C) of the innermost borehole to the lowest value of the outermost borehole. The outlet temperature T_o (thin line) can be distinguished only for the last borehole in the loop since it is the only one in which the outlet temperature does not coincide with the inlet temperature of the previous borehole in the chain. For borehole in parallel (figure 3), all the inlet temperatures T_i coincide (and only one of them can be displayed) but we can appreciate each single outlet temperature T_o (thin lines). The borehole temperatures T_b are displayed using a scatter plot. By comparing the temperature plots for series and parallel, we can notice how the series configuration induces greater radial stratification in the BTES temperatures. Regarding heat rates, a few observations can be done. First of all, the power exchanged for series arrangement is significantly lower when compared to the relative parallel cases. In parallel arrangement, the heat rate during heat injection is for the most part exchanged by the outermost boreholes. While for the series case, the heat rate during heat injection is initially mostly exchanged in the center and decreases with time until the largest portion of heat is rejected to the outermost boreholes. Table 3 shows that for the cases investigated the yearly mean extraction temperature is up to 4.5 °C higher for borehole connected in series compared to borehole in parallel. These values are much larger when we consider the monthly values (figure 8b). The table also shows that the mean storage temperature is up to 2 °C higher for parallel connections. This result is due to the larger amount of net power exchanged with these configurations. The improvement in grouting material in cases 3 and 4 results in slightly higher outlet temperatures. On the other hand the increase in flow reduces the outlet temperature during extraction but at the same time increases up to 1.5°C the average storage temperature since the net heat exchanged is increased. For the calculation of the mean storage temperature (equation 11), we used the procedure described in section 2.4. We considered ϵ equal to 0.01, a discharging time τ_d of 6 months and solved equation 13. The solution yields an r_ϵ of 17.54 m, which was utilized to build the domain $V_{\epsilon 1,\tau d}$. Figure 8a displays the domain area (~2954.27 m^2) and the discretization utilized for the numerical integration procedure.

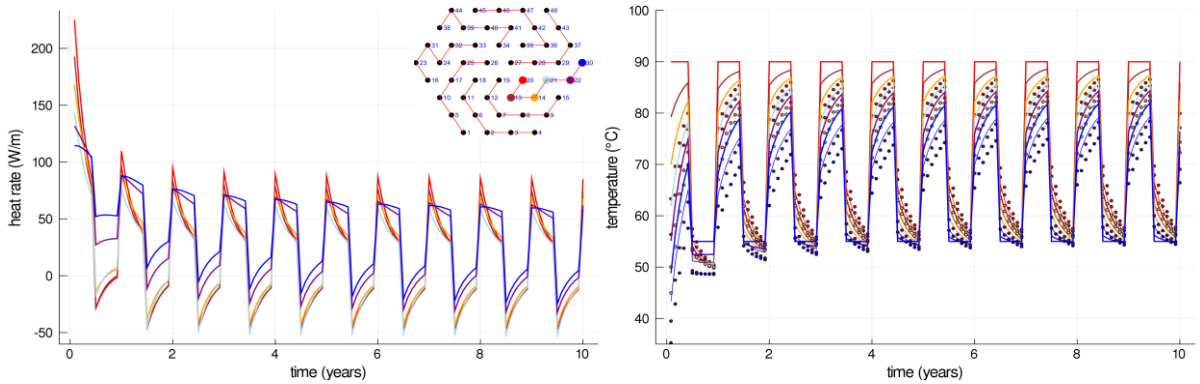

Figure 2: heat rate and temperature plots for case 0. A bore field map is used to display the color code used for displaying results of heat rate and temperature for selected boreholes. In the temperature plot, inlet temperatures T_i are displayed with thick solid lines, outlet temperature T_o with thin solid lines and borehole temperatures T_b using a scatter plot.

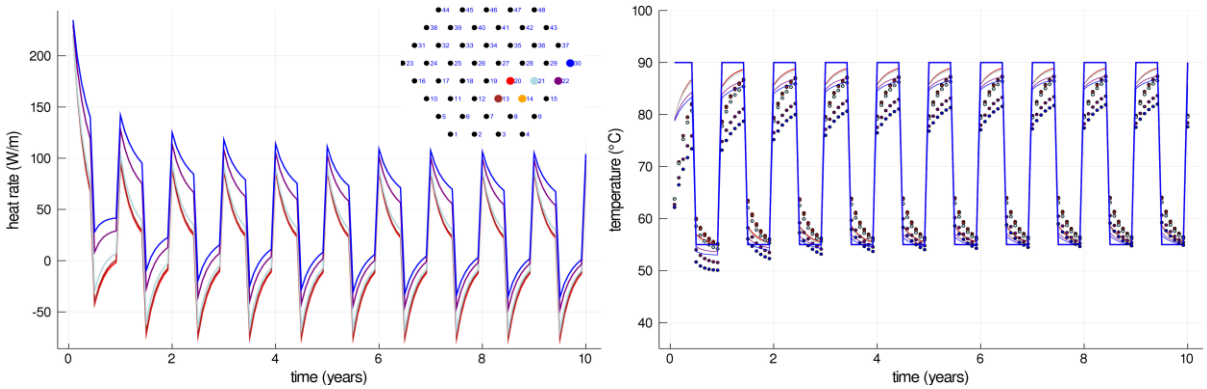

Figure 3: heat rate and temperature plots for case 1.

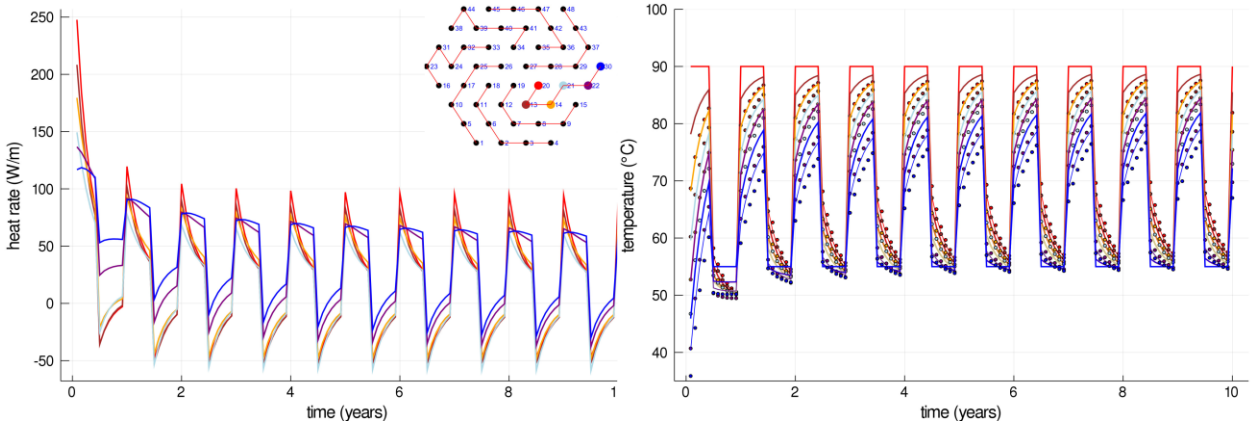

Figure 4: heat rate and temperature plots for case 2.

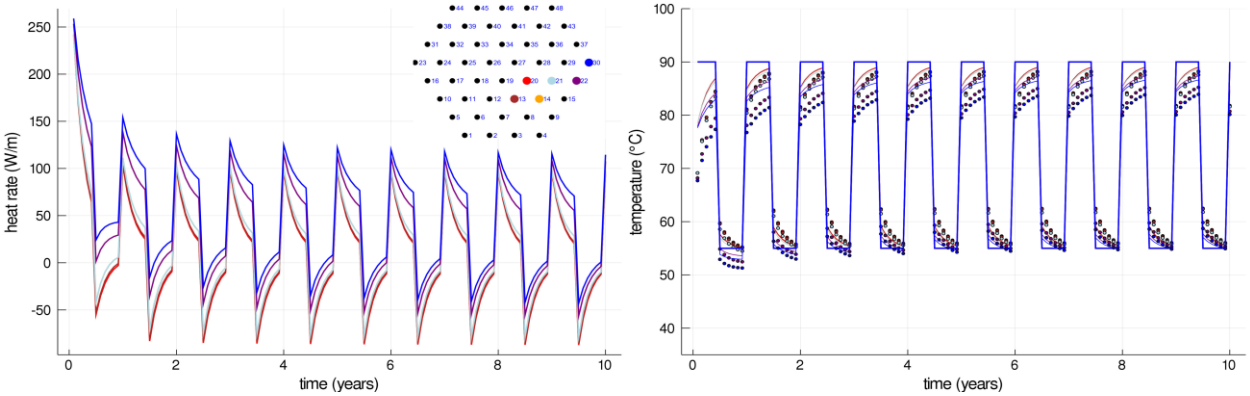

Figure 5: heat rate and temperature plots for case 3.

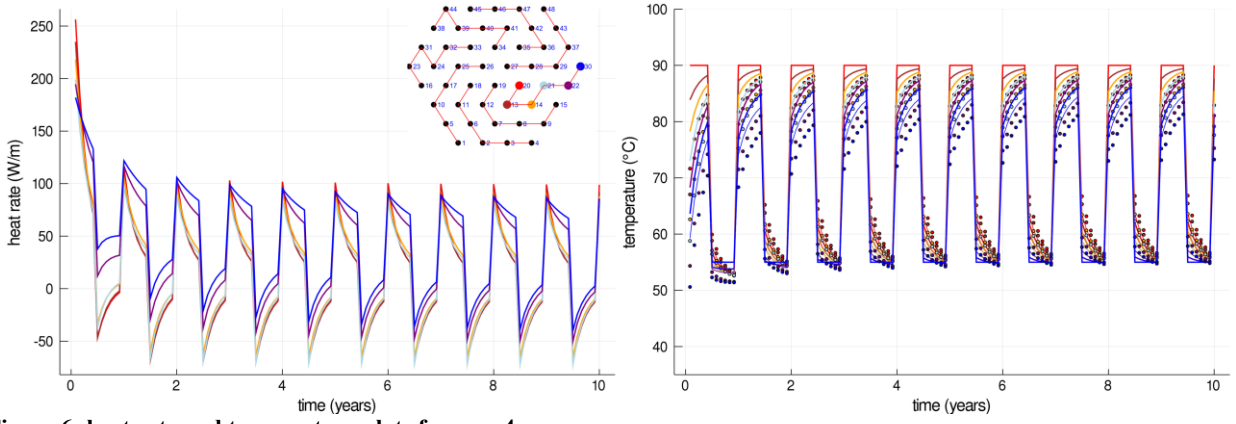

Figure 6: heat rate and temperature plots for case 4.

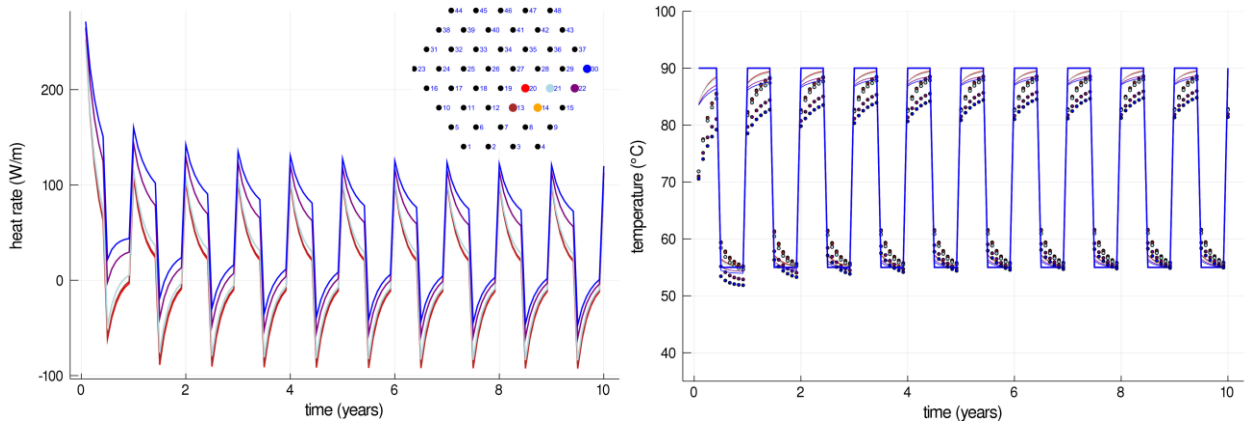

Figure 7: heat rate and temperature plots for case 5.

Table 3: yearly mean outlet temperatures during injection and extraction and yearly mean temperature of the storage, evaluated after 10 year of operation.

case	$\bar{T}_{out,inj}^{(year10)}$(°C)	$\bar{T}_{out,ext}^{(year10)}$(°C)	$\bar{T}_{storage}^{(year10)}$(°C)
0	75.3	60.3	45.1
1	87.1	56.2	47.1
2	74.6	60.9	45.5
3	86.9	56.4	47.6
4	81.4	58.7	46.8
5	88.4	55.7	47.9

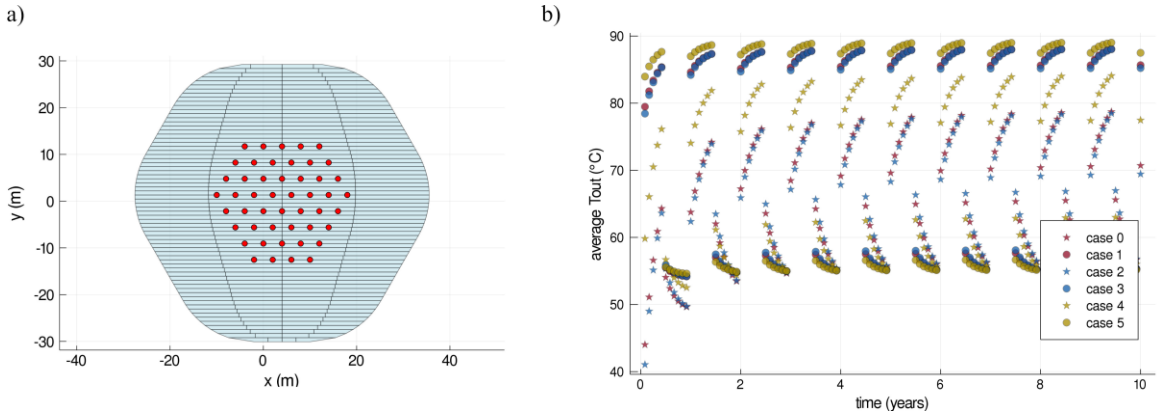

Figure 8: a) Storage domain V_{ϵ_1,τ_d} obtained considering ϵ equal to 0.01. The plot show also the discretization utilized for the numerical the integrations evaluated on V_{ϵ_1,τ_d}. b) mean outlet temperatures from the loops for each of the study cases.

3.2 Energy analysis

Energy flows injected and extracted from the BTES were calculated along with the energy stored in the BTES domain. Efficiencies were calculated as described in section 2.3. Table 4 and 5 show the values obtained for a number of relevant quantities after 10 years of operation for the 6 study cases investigated.

The results show that under the considered operational strategy (constant mass flow rate per branch and constrained input temperature), systems in parallel arrangement can extract and inject a significantly higher amount of heat than the series arrangement. The series arrangement is supplied with 1/6 of the mass flow and in order to achieve the same heat exchange would have to reach a temperature difference between inlet and outlet of the chain equal to 6 time the ΔT in a single borehole for the parallel arrangement case. This condition does not occur for the simulated cases. As seen in section 3.1, the increased energy extraction obtained with parallel arrangement comes at the cost of a lower extraction temperature. Improvement in the grouting material is beneficial and can highly improve the energy extracted. Further increase in the extraction/injection performance can be achieved by increasing the flow rate.

The difference in the net heat exchanged between the two arrangements is still in favor of parallel but it is less pronounced compared to the difference in extraction rate. As a consequence, the difference in heat stored within the storage volume is relatively low for the

6 cases considered (figure 9). As seen in section 3.1 this difference corresponds to a variation of around 2 °C in the mean temperature of the storage volume.

Figure 10 shows the seasonal efficiency and the storage efficiencies as a function of time. The first figure measure the performance in exchanging heat with the storage while the second figure assess the performance of the storage in maintaining the heat within the storage volume. The two plots shows opposite trends. While the efficiency η increases in time, the efficiency $\eta_{V\epsilon}$ decreases in time. This fact is depicted in figure 11. As time increases, the temperature within the borehole storage increases easing the process of extracting energy at high temperature. On the other hand, more and more energy diffuses across the BTES boundary and therefore is not recoverable under the current operation. Another observation that can be done by looking at Figure 10 is that there is a significant gap in seasonal efficiencies between the various solutions investigated. The gap in energy efficiency is readily explained by the inability of the series connected borehole to exchange as much energy as the parallel configurations. Increasing the flow by a factor 2 helps mitigating this issue and reducing this gap.

The values of seasonal energy efficiencies η obtained in the simulations are in a range that is comparable to the ones that have been observed in real installations operating at medium to high temperature with similar total borehole length. An example is the Drake Landing Solar Community in Canada with measured $\eta^{(\text{year10})}$ of 0.54 and a minimum extraction temperature of about 40 °C (Mesquita et al. 2017).

Table 4: Results of energy analysis evaluated after 10 year of operation.

case	$Q_{in}^{(year10)}/H$ (MWh/m)	$Q_{out}^{(year\ 10)}/H$ (MWh/m)	$Q_{exchanged}^{(tot)}/H$ (MWh/m)	$Q_{stored,\ V\epsilon1}$ (MWh/m)	$Q_{stored,\ V\infty}$ (MWh/m)	$\eta^{(year\ 10)}$	$\eta_{stored,\ V\epsilon1}$	$\eta_{stored,\ V\epsilon\infty}$
0	10.765	3.924	104.627	55.560	104.627	0.364	0.531	1
1	12.685	5.527	111.930	58.568	111.930	0.436	0.523	1
2	11.244	4.363	105.852	56.051	105.852	0.388	0.530	1
3	13.392	6.172	113.697	59.292	113.697	0.461	0.521	1
4	12.552	5.480	110.459	57.944	110.459	0.437	0.525	1
5	13.732	6.483	114.525	59.635	114.525	0.472	0.521	1

Table 5: Results of energy in terms of percentage change compare to reference case 0

case	$Q_{in}^{(year10)}/H$	$Q_{out}^{(year\ 10)}/H$	$Q_{exchanged}^{(tot)}/H$	$Q_{stored,\ V\epsilon1}$	$Q_{stored,\ V\infty}$	$\eta^{(year\ 10)}$	$\eta_{stored,\ V\epsilon1}$	$\eta_{stored,\ V\epsilon\infty}$
1	+17.83	+40.85	+6.97	+5.41	+6.97	+19.53	-1.46	+0
2	+4.45	+11.19	+1.17	+0.88	+1.17	+6.45	-0.28	+0
3	+24.40	+57.28	+8.66	+ 6.71	+8.66	+26.42	-1.79	+0
4	+16.59	+39.67	+ 5.57	+4.29	+5.57	+19.78	-1.21	+0
5	+27.56	+65.22	+9.46	+7.33	+9.46	+29.51	-1.94	+0

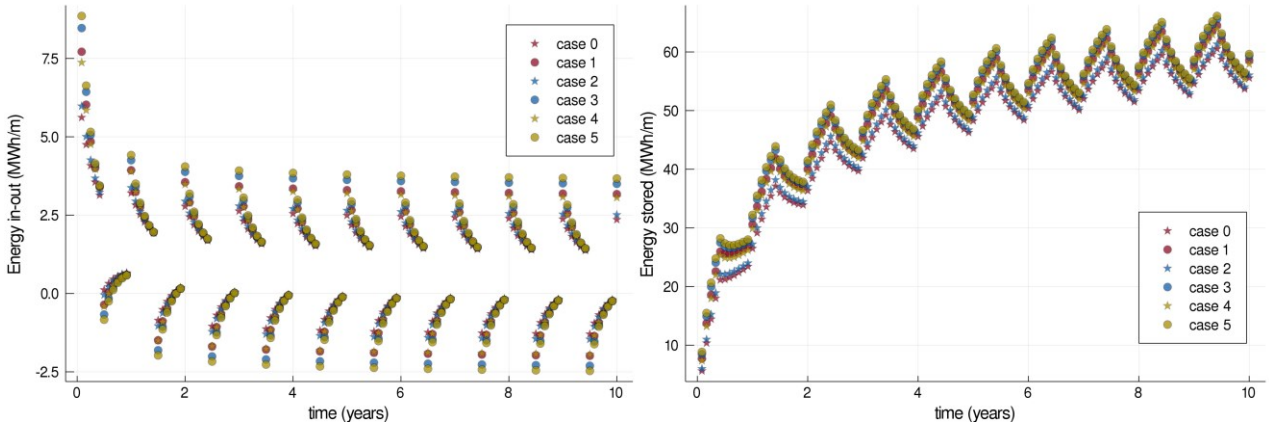

Figure 9: Energy injected and extracted and energy stored within the control volume $V\epsilon_1$.

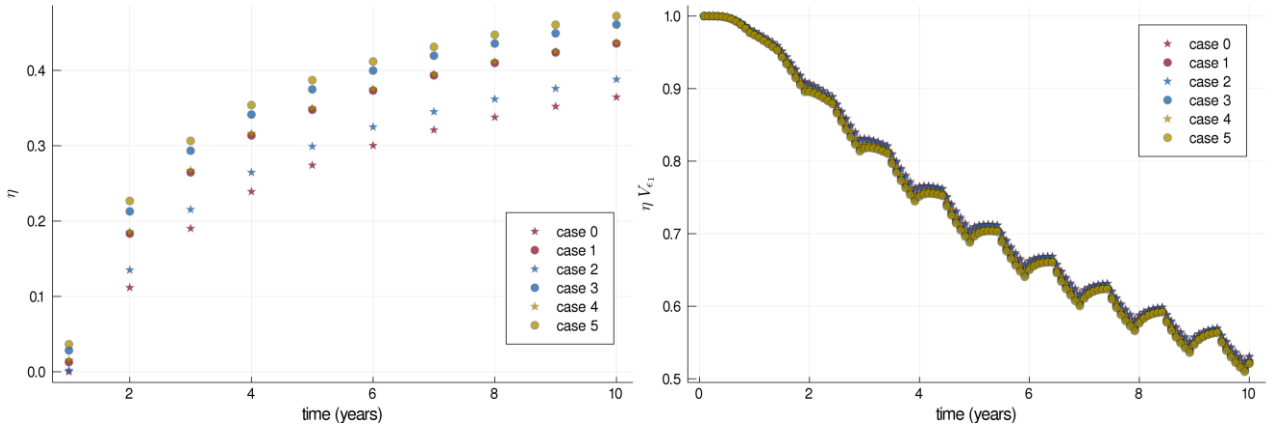

Figure 10: Seasonal energy efficiency η and storage energy efficiency $\eta_{V\epsilon1}$.

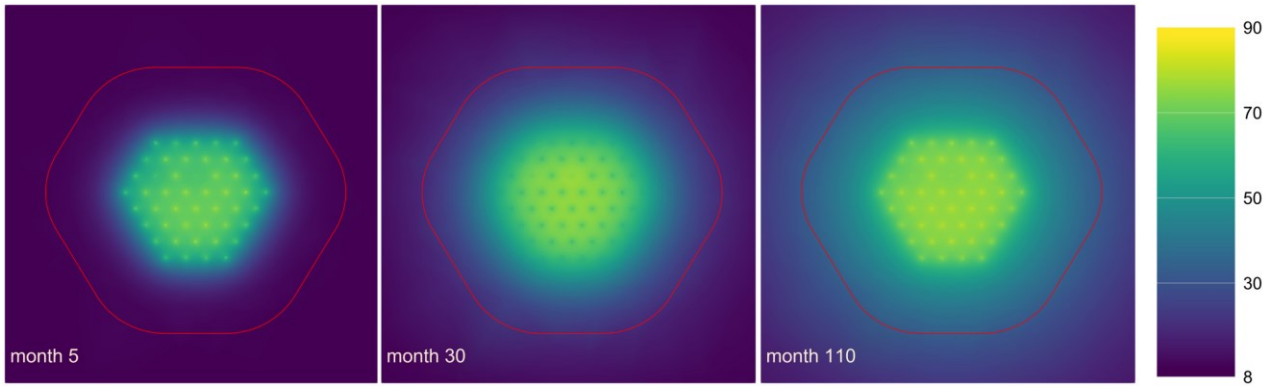

Figure 11: Evolution of the temperature field (in °C) during the operation of the BTES. The red line is the borehole storage boundary considering that maximum 1% of the heat outside this region can be recovered by the boreholes under the current operation.

3.3 Exergy analysis

Analogous parameters to the ones just presented in section 3.2 were calculated also in terms of exergy. Table 6 and 7 show the values obtained for each of the relevant quantities after 10 years of operation in the various study cases investigated. Similarly to what already observed in the energy analysis section, the exergy extracted in the BTES is significantly larger for systems in parallel arrangement with comparable mass flow rate per branch. Improvement in the heat exchanger and increase in flow increase these figures.

Regarding exergy efficiencies, Figure 13 shows that the spread in the values of seasonal exergy efficiencies in the different cases is much lower compared to the spread observed in figure 10 for energy efficiencies. This result reflect the fact that although the series BTES exchanges a lower amount of power compared to the parallel BTES, it injects this heat at a lower temperature and extract it at a higher temperature exploiting the stratification in the storage.

Another observation that can be done is that the exergy efficiency of the storage shows more significant variations compared to the energy efficiency of the storage which was almost indistinguishable between the different cases. The configurations connected in parallel yields a $\psi_{\text{stored, V}\epsilon1}$ that is around 10% lower compared to series configuration. This reflects the fact that injection of higher temperature heat in the outer boreholes results in higher exergy losses and that the better stratification obtained in the storage contribute in reducing exergy destruction. This cannot be observed in the energy losses $\eta_{V\epsilon1}$.which give very similar values for all the configurations.

Figure14 summarize the results for both seasonal efficiencies and storage efficiencies at 10th year of operation. The figure clearly shows that higher values of η do not necessarily corresponds to lower losses from the storage volume. In fact the configuration yielding the lowest seasonal energy and exergy efficiencies is also the one retaining the highest exergy storage efficiency $\psi_{\text{stored, }V\epsilon1}$. This example shows how using several parameters to analyze and compare different BTES configurations can improve the understanding of the system and provide insight to improve the design.

Table 6: Results of exergy analysis evaluated after 10 year of operation.

case	$Ex_{in}^{(year10)}/H$ (MWh/m)	$Ex_{out}^{(year10)}/H$ (MWh/m)	$Ex_{exchanged}^{(tot)}/H$ (MWh/m)	$Ex_{stored,\ V\epsilon1}$ (MWh/m)	$Ex_{stored,\ V\infty}$ (MWh/m)	$\psi^{(year\ 10)}$	$\psi_{stored,\ V\epsilon1}$	$\psi_{stored,\ V\epsilon\infty}$
0	2.251	0.598	22.572	3.592	4.406	0.266	0.159	0.195
1	2.822	0.804	27.864	3.947	4.895	0.285	0.142	0.176
2	2.341	0.670	22.858	3.650	4.486	0.286	0.160	0.196
3	2.976	0.901	28.676	4.038	5.020	0.303	0.141	0.175
4	2.709	0.822	26.020	3.875	4.795	0.303	0.149	0.184
5	3.075	0.938	29.539	4.083	5.079	0.305	0.138	0.172

Table 7: Results of exergy analysis in terms of percentage change compare to reference case 0.

case	$Ex_{in}^{(year10)}/H$	$Ex_{out}^{(year10)}$	$Ex_{exchanged}^{(tot)}/H$	$Ex_{stored,\ V\epsilon1}$	$Ex_{stored,\ V\infty}$	$\psi^{(year\ 10)}$	$\psi_{stored,\ V\epsilon1}$	$\psi_{stored,\ V\epsilon\infty}$
1	+ 25.37	+34.57	+23.44	+9.88	+11.09	+7.33	-10.98	-10.0
2	+ 4.01	+12.01	+1.26	+1.62	+1.81	+7.68	+0.35	-0.54
3	+32.20	+50.64	+27.04	+12.43	+13.92	+13.94	-11.50	-10.34
4	+20.36	+37.53	+15.27	+7.87	+8.82	+14.26	-6.42	-5.60
5	+36.62	+56.88	+30.86	+13.66	+15.28	+14.82	-13.14	-11.9

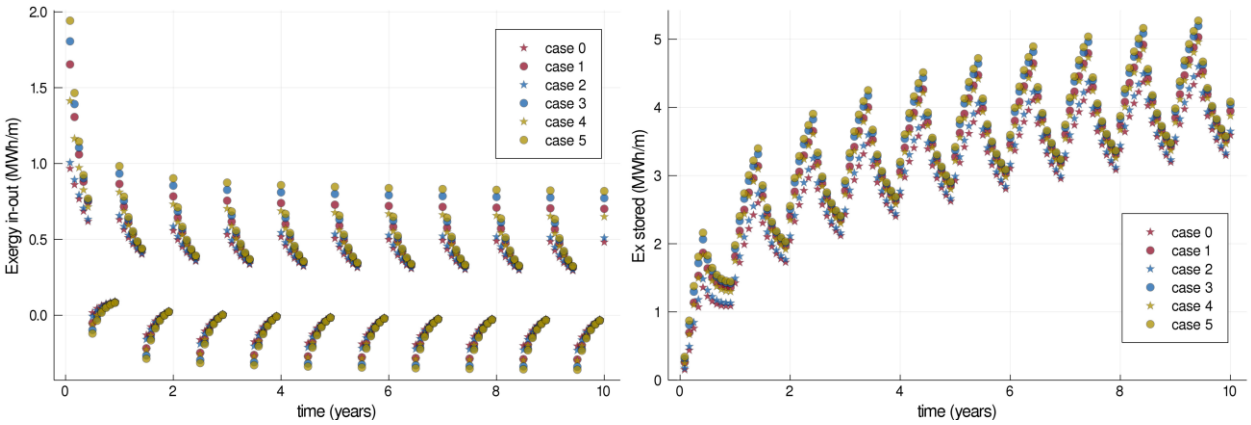

Figure 92: Exergy injected and extracted and exergy stored within the control volume $V\epsilon_1$.

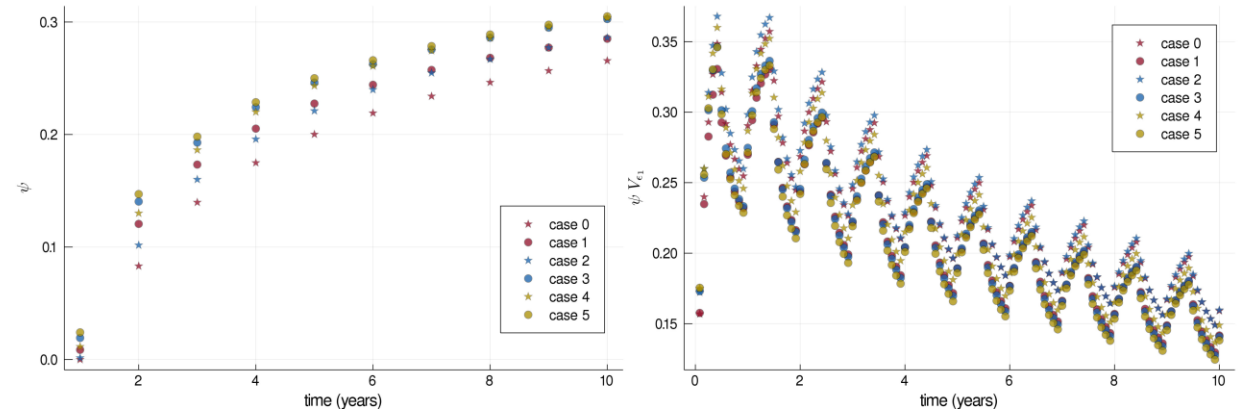

Figure 13: Seasonal exergy efficiency η and storage exergy efficiency $\eta_{V\epsilon1}$.

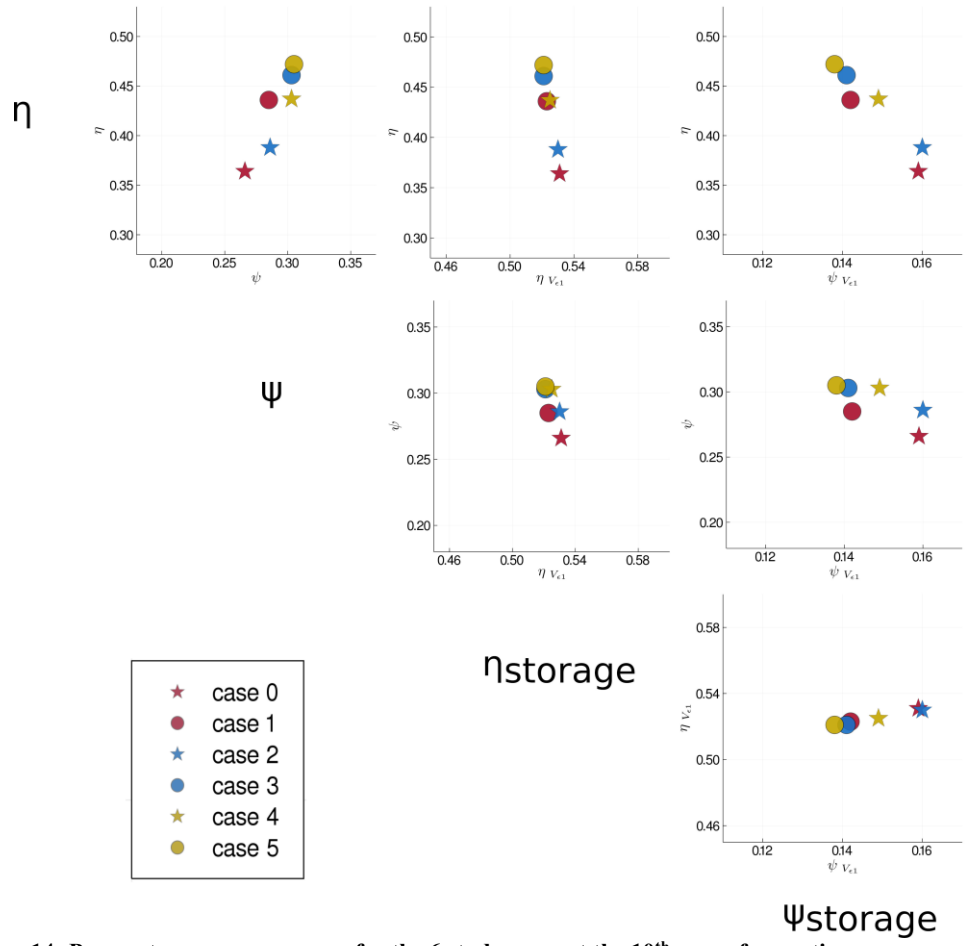

Figure 14: Parameters η, ψ, $\eta_{V\epsilon 1}$, $\psi_{V\epsilon 1}$, for the 6 study cases at the 10th year of operation.

3.4 Limitations of the current approach

The results showed in this paper are calculated using the ILS solution to model the ground. This approach eases the process of numerical integration which was necessary to compute some of the performance indicators investigated in this paper. On the other hand, the ILS solution is known to present a significant deviation in the long term thermal behavior compared to three dimensional models such as the Finite Line Source, since it does not account for heat transfer in the axial direction. For these reasons, the results shown in this paper should not be taken as absolute figures of the actual behavior of the system. Instead they should be seen as qualitative results that are used to display the potential use of the considered indicators to evaluate performance of the system but also to better understand its behavior.

4. CONCLUSIONS

The comparison of BTES systems with different configurations and different operating conditions is a non-trivial problem. The seasonal energy efficiency η is the most utilized parameters for this task. Although η is indeed a very important parameter, it is not sufficient to fully characterize the system operation and performance.

A first step into investigating a viable methodology for performance analysis of high temperature BTES systems has been presented in this paper. We explored the use of figures based on temperature, energy, and exergy and we evaluated these parameters as inlet and outlet quantities but also within the storage volume.

In order to test this approach, a BTES model based on classical analytical solution was developed, along with methods to compute energy stored, exergy stored in the ground storage control volume.

The method was illustrated with the help of 5 study cases built upon a reference case where the boreholes are connected in series and each borehole loop uses constant mass flow rate, with fluid circulation going from the center to the outer region during injection and in the opposite direction during extraction (injection and extraction temperatures of 90 °C and 55 °C, respectively). The reference temperature was chosen to be equal to the undisturbed ground level and control volume around the boreholes was chosen in such a way that that it contains a percentage of the overall heat injected after a time corresponding to the time for the discharge cycle. The borehole arrangement (series/parallel) were varied and mass flow rate and grout thermal conductivity were increased in the study cases.

The study cases investigated helped highlighting the richness of the system behavior and how a single parameter can hardly fully characterize the performance of the system.

5. ACKNOWLEDGMENTS

The authors of this paper would like to thank Energiforsk and the Swedish Energy Agency for financing this work through the research program Termiska Energilager.

REFERENCES

Aneke, M.: Wang, M. Energy storage technologies and real life applications – A state of the art review. *Applied Energy* **179**, (2016) 350–377.

Chu, S., Majumdar, A., 2012. Opportunities and challenges for a sustainable energy future. Nature 488, 294–303. https://doi.org/10.1038/nature11475

Cimmino, M.: G-functions for bore fields with mixed parallel and series connections considering axial fluid temperature variations, in: Proceedings of the IGSHPA Research Track (2018).

Cimmino, M.: Fluid and borehole wall temperature profiles in vertical geothermal boreholes with multiple U-tubes. *Renewable Energy* **96**, Part A, (2016), 137–147 .

Dincer, I., Rosen, M.: Thermal Energy Storage: Systems and Applications, 2nd ed. Wiley (2010).

Dunn, B., Kamath, H., Tarascon, J.-M., 2011. Electrical Energy Storage for the Grid: A Battery of Choices. Science 334, 928–935. https://doi.org/10.1126/science.1212741

Gehlin, S: Borehole thermal energy storage, in: Rees, S.J. (Ed.), Advances in Ground-Source Heat Pump Systems. Woodhead Publishing, (2016) pp. 295–327.

Jack, M.W., Wrobel, J., 2009. Thermodynamic optimization of a stratified thermal storage device. *Applied Thermal Engineering* **29**, (2009), 2344–2349.

Kallesøe, A.J. et al: HEATSTORE Underground Thermal Energy Storage (UTES) – state-of-the-art, example cases and lessons learned (2019).

Kizilkan, O., Dincer, I.:. Exergy analysis of borehole thermal energy storage system for building cooling applications. *Energy and Buildings* **49**, (2012), 568–574.

Lazzarotto, A.: A network-based methodology for the simulation of borehole heat storage systems. *Renewable Energy* **62**, (2014), 265–275.

Malmberg, M., Mazzotti, W., Acuña, J., Lindståhl, H., Lazzarotto, A: High temperature borehole thermal energy storage - A case study, in: Proceedings of the IGSHPA Research Track (2018).

Mesquita, L., McClenahan, D., Thornton, J., Carriere, J., Wong, B.: Drake Landing Solar Community: 10 years of operation, in: Proceedings of the ISES Solar World Congress 2017, Abudabi, (2017).

Mohd, A., Ortjohann, E., Schmelter, A., Hamsic, N., Morton, D., 2008. Challenges in integrating distributed Energy storage systems into future smart grid, in: 2008 IEEE International Symposium on Industrial Electronics. Presented at the 2008 IEEE International Symposium on Industrial Electronics, pp. 1627–1632. https://doi.org/10.1109/ISIE.2008.4676896

Moriarty, P., Honnery, D., 2016. Can renewable energy power the future? Energy Policy 93, 3–7. https://doi.org/10.1016/j.enpol.2016.02.051

Pickard, W.F., 2014. Smart Grids Versus the Achilles' Heel of Renewable Energy: Can the Needed Storage Infrastructure Be Constructed Before the Fossil Fuel Runs Out? Proc. IEEE 102, 1094–1105. https://doi.org/10.1109/JPROC.2014.2316359

Rosen, M.A., Dincer, I.: 2003. Exergy methods for assessing and comparing thermal storage systems. *International Journal of Energy Research* **27**, (2003) 415–430

Rosen, M.A., Tang, R., Dincer, I.: 2004. Effect of stratification on energy and exergy capacities in thermal storage systems. International Journal of Energy Research **28**, (2004) 177–193.

Sliwa, T., Rosen, M.A.:. Efficiency analysis of borehole heat exchangers as grout varies via thermal response test simulations. Geothermics 69, 132–138. (2017).

Tordrup, K.W., Poulsen, S.E., Bjørn, H.: An improved method for upscaling borehole thermal energy storage using inverse finite element modelling. Renewable Energy 105, 13–21. (2017)